A Feedback Linearization Controller Applying Multi-Layer Perceptron and Wavelet Neural Networks into a Hydraulic Actuator

Fabio A. P. Borges[1][0000-0002-6847-3205], Thomaz P. Silva Jr.[1][0000-0001-6923-3775], Letieri R. De Ávila[1][0009-0000-4000-9219], and Vitor M. Fiori[1][0000-0002-2856-5164]

Federal University of Rio Grande, N2E Research Group, Engineering School, Rio Grande, Brazil
fborges@furg.br
hbkthomaz@gmail.com
letieriavila@gmail.com
vmfiori@hotmail.com

Abstract. In this paper, a design method applied to a hydraulic actuator is proposed. The method comprises a feedback linearization-based controller with friction compensation and estimation of the inversion term. Although very effective and with strong stability guarantees, feedback linearization control depends on parameters that are difficult to determine, requiring large amounts of experimental effort to be identified accurately. On the other hand, neural networks require little effort regarding the parameter identification of the control hardware. Offline-trained multi-layer perceptron and wavelet neural networks are applied in the present work, simplifying the controller in comparison with other similar online strategies. Lyapunov-based analysis is applied to obtain the formal stability proof of this strategy. The effectiveness of the proposed method is verified by means of simulation and experimental results where low and high disturbances in the load are considered. The results confirm that the method is effective in the absence of a high disturbance in the load.

Keywords: Hydraulic control · Neural networks · Multi-layer perceptron · Wavelet networks

1 Introduction

Hydraulic actuators are widely applied in industrial tasks that combine high forces with reduced dimensions. Despite such benefits, they have some important drawbacks when high precision is required in their dynamic responses. Strong nonlinearities present in the dynamic model of the hydraulic actuators, such as the friction force in the piston and the hydraulic valve response [1], turn a controller design that can drive a precise response against such characteristics into a challenging task. Control strategies that use nonlinear model-based controllers combined with online learning algorithms have been proposed in more recent works to overcome the nonlinearities and parametric uncertainties of the model. The backstepping strategy has been applied in conjunction with the Extended Disturbance Observer (EDO) [2], Extended Differentiator [3], and Extended State Observer (ESO) [4]. Sliding mode control is applied in [5–7] and feedback linearization-based controllers in [8–10]. We can observe in such works a reduced position error in comparison with the traditional PID controllers and a convergence of the uncertain parameters present in the model by the use of adaptive techniques based on Lyapunov methods that aim to obtain stability in the closed loop system. Despite such satisfactory results, they also have important drawbacks for practical applications. In the mentioned strategies, a large number of control parameters must be tuned, where a compromise between the robustness of the controller, the computing capabilities of the available control hardware, and the convergence speed of the estimation procedure must take into account, which turns the tuning process rather difficult and sometimes demand sophisticated hardwares. Moreover, the sensor noise is critical for the convergence performance in online strategies and may require expensive devices for a satisfatory result.

In the present work, we propose a control scheme applied to a hydraulic positioning system, introduced in [11], where two control loops, based on the main phenomena involved in the system are designed: the outer loop encompasses the mechanical variables, whereas the inner loop uses a feedback linearization strategy, which aims at compensating for the nonlinearities due to the hydraulic dynamics. In the outer loop, we use a static neural network to compensate for the nonlinear effect of the friction forces in the piston. In the inner loop, we use a neural network to compute the inversion term required in the feedback linearization strategy. Two different classes of neural networks are proposed to be applied in the static neural network that compounds the proposed controller: Multi-layer perceptron, which was successfully applied in [11], and wavelet neural networks. According to [12], wavelet neural networks are a class of RBF neural networks that have important advantages when compared with the traditional RBF and feedforward multi-layer perceptron neural networks, such as a better generalization capability for networks with reduced input dimension, a linear relation between the hidden and output layers and an analytical methodology for the initialization of the parameters in the core of hidden layer. In the present work, the neural network´s parameters are acquired by extensive offline training. The offline training procedure reduces significantly the computing efforts involved in the control strategy, thus requiring control hardwares simpler than those applied for fully online-trained controllers. The efectiveness of the proposed strategy is demonstrated both analitically, with a rigorous stability proof using Lyapunov's Second Method, and with comprehensive simulation and experimental results. The results obtained with multi-layer perceptron and wavelet neural networks are compared. Finally, the better configuration is applied in a experimental plant. Despite the good results obtained in [11] with respect to the same strategy, in such previous work an analisis of the load disturbance effects was not performed. Moreover, in the present work we propose the compensation of the friction force in the piston and present the statibity formal proof considering such control action. The use of RBF networks is usual in several papers in hydraulic control. In the present work we use the powerfull wavelet networks as an alternative to MLP networks.

The remainder of this paper is structured as follows. In Section 2, the hydraulic actuator model is discussed. In Section 3, we present the overall control strategy, whereas Sections 4, 5, and 6 are dedicated to the development of the proposed neural networks. In Section 7, the stability proof is detailed, while, in Section 8, the proposed method is evaluated by means of simulation and experimental results. Finally, the main conclusions are outlined in Section 9.

2 System Model

We may observe by means of Figure 1 the hydraulic actuator applied in the present work, composed of a differential cylinder that is attached to a load. The parameters illustrated in Figure 1 are described in Table 1 and along the present section. Figure 2 represents the experimental setup.

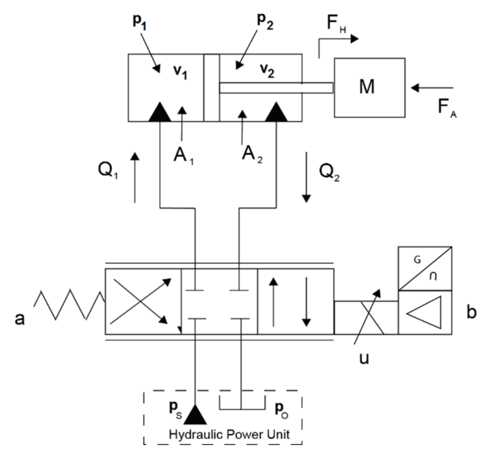

Fig. 1. Schematic description of the hydraulic actuator.

According to Newton's Second Law and flow-continuity considerations, as described in detail in [1], the equations representing the system dynamics are:

$$M\ddot{y} + F_A = F_H - F_D \tag{1}$$

$$\dot{p}_1 = \frac{\beta}{v_1 + A_1 y} \left(Q_1 - A_1 \dot{y}\right) \tag{2}$$

$$\dot{p}_2 = -\frac{\beta}{v_2 - A_2 y} \left(Q_2 - A_2 \dot{y}\right) \tag{3}$$

Table 1. System parameters.

Parameter	description	Value
v_1	Chamber volume 1	$1.2446 \times 10^{-4} m^3$
v_2	Chamber volume 2	$9.9060 \times 10^{-5} m^3$
$K_{v1}; K_{v2}$	Volumetric flow rates gains	$\sqrt{2} \cdot 15.11 \times 10^{-9} m^3/(s \times \sqrt{Pa})$
l_1	Pressure loss 1	$5.68 \times 10^{10} Q_1 Pa$
l_2	Pressure loss 2	$4.35 \times 10^{10} Q_2 Pa$
l_3	Pressure loss 3	$3.59 \times 10^{10} Q_1 Pa$
l_4	Pressure loss 4	$3.59 \times 10^{10} Q_2 Pa$
M	Load mass	$14.54 kg$
A_1	Chamber area 1	$4.91 \times 10^{-4} m^2$
A_2	Chamber area 2	$2.37 \times 10^{-4} m^2$
β	Bulk modulus	$1.0 \times 10^9 N/m^2$
P_s	Supply pressure	$50 \times 10^5 Pa$
P_0	Reference pressure	$0 Pa$

Fig. 2. Experimental setup.

y, $\dot{y}$ and $\ddot{y}$ are the position, velocity, and acceleration of the piston-load assembly, respectively. p_1 and p_2 are the pressure chambers. Q_1 and Q_2 are the volumetric flow rates. $F_H = p_1 A_1 - p_2 A_2$ is the hydraulic force applied to the piston. β is the bulk modulus. F_D represents a generic disturbance force.

The volumetric flow rates through the valve orifices are functions of the pressures in the chambers and the input signal applied to the valve, expressed by:

$$
\begin{aligned}
Q_1 &= K_{v1} u g_1,\ g_1 = \begin{cases} \sqrt{p_s - (p_1 + l_1)}, & u \geq 0 \\ \sqrt{p_1 - l_3}, & u < 0 \end{cases} \\
Q_2 &= K_{v2} u g_2,\ g_2 = \begin{cases} \sqrt{p_2 - l_4}, & u \geq 0 \\ \sqrt{p_s - (p_2 + l_2)}, & u < 0 \end{cases}
\end{aligned} \tag{4}
$$

K_{v1} and K_{v2} are the flow rate gains that characterize each orifice of the valve, whereas $l_1 ... l_4$ are the pressure losses caused by the hydraulic line couplers, which are significant and must be taken into account when high-precision tasks are considered.

Equations 1-4 form an open-loop model of the system. The values of its parameters are given in Table 1. The experimental effort to acquire the model parameters is described in detail in [13].

3 Proposed Controller

Feedback linearization is the control strategy applied in the present work. The system model can be written in the so-called control/input affine form, i.e.:

$$x^{(n)} = f(x) + b(x)u \tag{5}$$

where u is a scalar control input, x is the scalar output of interest, $\boldsymbol{x} = [x, \dot{x}, ..., x^{n-1}]$ is the state vector, and $f(\boldsymbol{x})$ and $b(\boldsymbol{x}) \neq 0$ are nonlinear state functions. If $f(\boldsymbol{x})$ and $b(\boldsymbol{x})$ are known, defining $v(\boldsymbol{x})$ as a linear term matching the desired dynamics for the closed-loop system, it is straightforward that the input

$$u = b^{-1}(x)[v(x) - f(x)] \tag{6}$$

leads the controlled nonlinear system to perform as a linear one that presents the desired dynamic behavior, i.e.:

$$x^{(n)} = v(x) \tag{7}$$

Considering the error between the estimated model and the system, the closed-loop dynamics can be written as

$$x^{(n)} = v(x) + \epsilon \tag{8}$$

where ϵ is the residue from imperfect cancellations.

The controller that we apply in the present work is based on interpreting the actuator as two interconnected subsystems:

– In the mechanical subsystem (outer loop), it is computed a first control law that represents a desired hydraulic force that leads the piston to track its position trajectory;
– In the hydraulic subsystem (inner loop), it is developed a second control law, which leads to tracking the desired hydraulic force value as closely as possible.

The control law applied to the mechanical subsystem is based on [14]. It is composed of a reference acceleration $\ddot{y}_r$ and an auxiliary error measure z, defined as follows:

$$\ddot{y}_r = \dot{y}_d - \lambda\tilde{y} \tag{9}$$

$$z = \dot{\tilde{y}} + \lambda\tilde{y} \tag{10}$$

where y_d is the desired piston position, $\tilde{y} = y - y_d$ is the position tracking error, and λ is a positive gain. All terms marked with one or two dots are the first or second time derivatives of the corresponding variables, respectively.

The desired force F_{Hd} is the output of the mechanical subsystem. The control law applied in the mechanical subsystem is given by:

$$F_{Hd} = M\ddot{y}_r - K_d z + \phi(\dot{y}, p_1, p_2) \tag{11}$$

where we use a static neural network $\Phi(\dot{y}, p_1, p_2)$ to compensate for the friction force F_A presented in Equation 1. K_d is a positive gain.

In the hydraulic subsystem, we use feedback linearization control. When all the terms are written in the form of Equation 5, one proceeds as follows. First, define $\boldsymbol{x} = [y, \dot{y}, F_H]^T$ and the auxiliary terms f_1 and f_2 as:

$$f_1 = \frac{\beta}{v_1 + A_1 y}, f_2 = \frac{\beta}{v_2 - A_2 y} \tag{12}$$

and replacing Q_1, Q_2, f_1, and f_2 in Equations 2 and 3 with their corresponding terms given in Equations 4 and 12. The dynamic for this subsystem is given by:

$$\dot{F}_H = -\left(A_1^2 f_1 + a_2^2 f_2\right)\dot{y} + \left(A_1 f_1 K_{v1} g_1 + A_2 f_2 K_{v2} g_2\right) u \tag{13}$$

Since the objective is to cancel its nonlinear effects and generate the desired force F_{Hd}, the proposed control law is:

$$u = \Omega\left(y, \dot{y}, p_1, p_2\right)\left[\dot{F}_{Hd} - K_p\tilde{F}_H + \left(A_1^2 + A_2^2 f_2\right)\dot{y}\right] \tag{14}$$

where $\dot{F}_{Hd}$ is the time derivative of the desired hydraulic force, $\tilde{F}_H = F_H - F_{Hd}$, and K_p is a positive feedback gain. We represented the term $b^{-1}(\boldsymbol{x})$ in Equation 6 by a static neural network $\Omega\left(y, \dot{y}, p_1, p_2\right)$.

4 Wavelet Neural Network

A wavelet family is a set of functions generated by means of the translation and dilatation of a mother wavelet ψ. The structure of the WNN used in the present work is similar to that applied in [12] and [15]. The network output, considering only one output, is given by the following expression:

$$y = \boldsymbol{W}_1 \boldsymbol{\Psi}(\boldsymbol{A}, \boldsymbol{B}, \boldsymbol{x}) + \boldsymbol{b}_w + \boldsymbol{W}_2 \boldsymbol{x} \tag{15}$$

where $\boldsymbol{W}_1$ is the weighting vector that connects the hidden layer to the output layer, $\boldsymbol{b}_w$ is the bias associated with the output layer, $\boldsymbol{W}_2$ is the weighting vector that connects the input vector $\boldsymbol{x}$ to the output layer, and $\boldsymbol{\Psi}(\boldsymbol{A}, \boldsymbol{B}, \boldsymbol{x})$ is the wavelons vector, computed according to the input vector $\boldsymbol{x}$ and the matrices of dilatations and translation $\boldsymbol{A}$ and $\boldsymbol{B}$.

If we worked with a WNN where the number of wavelons is m, i.e., the number of hidden nodes, and the number of inputs is p, the expression in Equation 15 can be written as:

$$y = \sum_{i=1}^{m} w_{1i} \Psi_i(A_i, B_i, \boldsymbol{x}) + b_w + \sum_{g=1}^{p} w_{2g} x_g \tag{16}$$

where:

$$\Psi_i(A_i, B_i, \boldsymbol{x}) = \prod_{j=1}^{p} \psi(z_{i,j}) \tag{17}$$

being that ψ is the mother wavelet chosen for the WNN. The scalar $z_{i,j}$ is given by:

$$z_{i,j} = \frac{x_j - B_{i,j}}{A_{i,j}} \tag{18}$$

Following [12], the Mexican Hat is the mother wavelet adopted in the present work. It is given by:

$$\psi(z_{i,j}) = \left(1 - z_{i,j}^2\right) e^{-\frac{1}{2} z_{i,j}^2} \tag{19}$$

5 Feedforward Multi-Layer Perceptron

The feedforward multi-layer perceptron (MLP) neural network is the most common approach for neural networks [16–18]. A matrixial representation is:

$$o = \boldsymbol{\Gamma}\left[\boldsymbol{W}_n \boldsymbol{\Gamma}\left[\boldsymbol{W}_{n-1} ... \boldsymbol{\Gamma}\left[\boldsymbol{W}_1 \boldsymbol{u} + \boldsymbol{b}_1\right] + ... + \boldsymbol{b}_{n-1}\right] + \boldsymbol{b}_n\right] \tag{20}$$

where $\boldsymbol{W}_n$ is the weighting matrix of the n-th layer, $\boldsymbol{b}_n$ is the bias vector associated with each layer node, and $\boldsymbol{\Gamma}(\boldsymbol{x}) = [\boldsymbol{\gamma}_1(\boldsymbol{x}, \boldsymbol{\gamma}_2(\boldsymbol{x}), ..., \boldsymbol{\gamma}_n(\boldsymbol{x})]$ is a nonlinear operator where each $\boldsymbol{\gamma}_n(.)$ is a monotonic and continuously differentiable activation function. In the present work, the sigmoidal logistic function is used.

6 Neural Network Training and Validation

The cross-validation method [19] is applied in the static neural networks training. The acquisition process of the training and validation sets is performed offline. With the purpose of acquiring representative sets, we use a simple proportional controller to lead the system to track the desired position trajectory described in Equation 21 and perform the measures of the pressure and position responses of the plant, applying such values in the training sets, as illustrated in Figure 3.

$$y_d = 0.1 + A \sin(\omega t) \tag{21}$$

where $A$is the amplitude and ω is the angular frequency. The amplitude is kept at a fixed value of 0.08 m.

In the proposed profile, the piston is moved by means of a set of sinusoidal trajectories where five different frequencies from 0.25 rad/s to 1 rad/s are applied in the training set and two different frequencies of 0.81 rad/s and 0.93 rad/s in the validation set. Such a procedure aims to ensure a smooth transition for the piston.

The Quickprop algorithm [20] is applied in the training process.

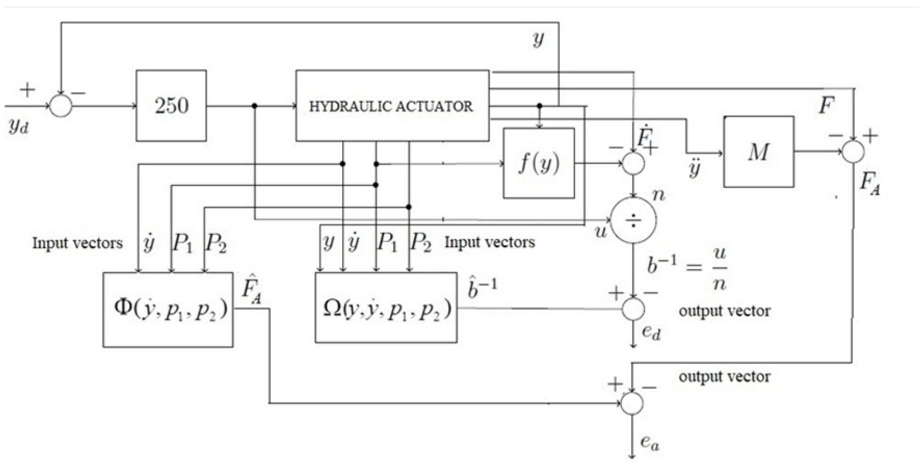

Fig. 3. Static neural networks: training and validation set generation.

7 Stability Analysis

For the stability analysis, the Lyapunov method was applied. The following assumptions are considered:

– The mechanical subsystem parameters are known, except for the friction force in the piston. The hydraulic subsystem parameters are subject to uncertainties.
– The desired piston position $y_d(t)$ and its time derivatives up to 3rd order are continuous bounded functions.
– The cancellation residue ϵ in 8 is rewritten in terms of a percentage error term δ, where we assume that $-1 < \delta \leq \bar{\delta}$. Whether the NN reproduces exactly the function b^{-1}, then $\delta = 0$.
– The error in the cancelation of the friction force by the NN is bounded and it is represented by ϕ.

Based on such assumptions, we can write 14 as:

$$u = \mathit{\Omega}\left(y, \dot{y}, p_1, p_2\right)[v + f] + \epsilon = b^{-1}\left[\dot{F}_{Hd} - K_p\tilde{F}_H + f\right](1 + \delta) \tag{22}$$

Considering the open-loop model of the system, given by Equations 1 and 13, and the proposed control structure, represented by Equations 11 and 22, substituting each proposed control law into the dynamics of its corresponding subsystem (11 into 1 and 22 into 13), the behavior of the closed-loop system can be described in terms of the following expressions:

$$M\dot{z} = -K_d z + \tilde{F}_H + F_D + \phi \tag{23}$$

$$\dot{\tilde{F}} = -K_p\tilde{F} + \delta\left[\dot{F}_{Hd} - K_p\tilde{F}_H + f\right] \tag{24}$$

Considering these expressions, the stability properties of the closed-loop system are proven as follows. Defining the trajectory tracking errors of the system in terms of the auxiliary vector $\boldsymbol{\rho} = \left[\tilde{y}\ \dot{\tilde{y}}\ \tilde{F}_H\right]^T$ and considering the closed-loop system dynamics described by Equations 23 and 24 subject to an unmodeled disturbance force F_D, upper-bounded by $\bar{F}_D$ and considering the model of the system subject to uncertainties whose combined effect can be represented as a percentage factor δ with an upper bound $\bar{\delta}$ and an error ϕ with an upper-bounded $\bar{\phi}$, the following affirmation is true:

Given an arbitrary initial condition, the controller gains can be chosen so as to ensure that the trajectory-tracking error vector $\boldsymbol{\rho}$ converges to a limited residual set R as $t \to \infty$. The amplitude of such a set depends on $\bar{\phi}$, $\bar{F}_D$, $\bar{\delta}$, and the controller's gains. Moreover, if $F_D = 0$ and the output of the wavelet networks used in the hydraulic and mechanical subsystems control law cancels uncertainty effects, then $\|\boldsymbol{\rho}\|$ as $t \to \infty$.

Consider the Lyapunov candidate function:

$$V = \frac{1}{2}\left(HMz^2 + P\tilde{y}^2 + \tilde{F}_H^2\right) \tag{25}$$

where P and H are positive constants. By taking the time derivative of 25, substituting into it the expressions 23 and 24, and considering $P = 2\lambda K_d H$ we obtain:

$$\dot{\boldsymbol{V}} = -\left(\boldsymbol{\rho}^T \left(\dot{\boldsymbol{N}}_2\right) \boldsymbol{\rho} + \boldsymbol{\rho}^T \boldsymbol{\Delta}\right) \tag{26}$$

$$\boldsymbol{N}_2 = \begin{bmatrix} \lambda^2 H K_d & 0 & -\frac{1}{2}H\lambda - \frac{\delta\alpha_1}{2} \\ 0 & HK_d & -\frac{1}{2}H - \frac{\delta\alpha_2}{2} \\ -\frac{1}{2}H\lambda - \frac{\delta\alpha_1}{2} & -\frac{1}{2}H - \frac{\delta\alpha_2}{2} & K_p - \delta\alpha_3 \end{bmatrix} \tag{27}$$

$$\Delta = \begin{bmatrix} \lambda H \left(F_D + \phi\right) \\ H \left(F_D + \phi\right) \\ \Psi_d \delta \end{bmatrix} \tag{28}$$

α_1, α_2, α_3, and Ψ_d are the following bounded auxiliary terms:

$$\alpha_1 = \left(\left(M\lambda + K_d\right) \frac{\lambda K_d}{M}\right) \tag{29}$$

$$\alpha_2 = \left(\left(M\lambda + K_d\right)\left(\lambda + \frac{K_d}{M}\right) - \lambda K_d + \left(A_1^2 f_1 + A_2^2 f_2\right)\right) \tag{30}$$

$$\alpha_3 = \left(-K_d \frac{1}{M} - \left(\lambda + K_p\right)\right) \tag{31}$$

$$\Psi_d = M\,\dddot{y}_d + \left(A_1^2 f_1 + a_2^2 f_2\right)\dot{y}_d + \dot{\phi}\left(\dot{y}, p_1, p_2\right) \tag{32}$$

Such terms were computed considering:

$$\dot{F}_{Hd} = \left(-K_d - M\lambda\right)\ddot{\tilde{y}} - K_d \lambda \dot{\tilde{y}} + M\,\dddot{y}_d + \dot{\phi}\left(\dot{y}, p_1, p_2\right) \tag{33}$$

$$\ddot{\tilde{y}} = -\lambda \dot{\tilde{y}} - M^{-1} K_d \left(\dot{\tilde{y}} + \lambda \tilde{y}\right) + M^{-1} \tilde{F}_H - M^{-1}\left(F_D + \phi\right) \tag{34}$$

From Equation 26, if $F_D = \phi = \delta = 0$, by applying the Sylvester Criterion, $K_d K_p > 1/2H$ is a sufficient condition to ensure that $\dot{\boldsymbol{V}}(t)$ is negative definite. Therefore, $\|\boldsymbol{\rho}\| \to 0$ as $t \to \infty$. But, if $\delta \neq 0$ and/or $F_D \neq 0$ and/or $\phi \neq 0$, by the same criterion, $\boldsymbol{N}_2$ can be made symmetric and positive definite if:

$$\begin{aligned} K_p >& \frac{1}{\left(\lambda^2 K_d H\right)\left(1+\delta\right)} \\ &\Rightarrow \left(\left(\frac{1}{2}H\lambda + \frac{\delta\alpha_1}{2}\right)^2 + \left(\frac{1}{2}H + \frac{\delta\alpha_2}{2}\right)^2 \lambda^2 + \lambda^2 K_d H \delta \left(K_d - \lambda M\right)\frac{1}{M}\right) \end{aligned} \tag{35}$$

where such condition is satisfied by choosing K_p as an appropriate value. With the feedback gains and parameter values presented in Section 6, and using $H = 9 \times 10^5$, the criterion defined in Equation 35 holds for $\bar{\delta} = 0.17$, which means that the stability condition holds for estimation errors up to $\pm 17\%$ in the output given by the static neural network. Within the region where this condition is met, application of the Rayleigh-Ritz Theorem combined with the Cauchy-Schwartz Inequality to Equation 26 yields:

$$\dot{\boldsymbol{V}} \leq -\lambda 2^T \|\rho\| \|\Delta\|_{min} \tag{36}$$

where $\lambda 2_{min}$ is the minimum eigenvalue of $\boldsymbol{N}_2$. Under the assumption that ϕ, F_D and δ are upper-bounded, and since Ψ_d has also an upper limit $\bar{\Omega}_d$ because it is derived from the desired trajectory, we have that $\|\Delta\|$ is upper-bounded by $\bar{\Delta} = \sqrt{\lambda^2 H^2 \left(\bar{F}_D + \bar{\phi}\right)^2 + H^2 \left(\bar{F}_D + \bar{\phi}\right)^2 + \bar{\delta}^2 \bar{\Psi}_D^2}$. Therefore, the condition $\dot{V}(t) < 0$ is attained if:

$$\|\rho\| > \frac{\bar{\Delta}}{\lambda 2_{min}} \tag{37}$$

From Equation 37, we can conclude that any system trajectory with initial condition $\boldsymbol{\rho}(0)$ that is outside a ball with a radius $\bar{\Delta}/\left(\lambda 2_{min}\right)$ must converge and remain confined to such ball as $t \to \infty$. Such a condition ensures that $\|\boldsymbol{\rho}(t)\|$ is a limited quantity. Moreover, in the absence of disturbances and if the action of the neural networks can overcome parametric uncertainties, we have $F_D = \delta = \phi = 0$ and the closed-loop tracking errors converge asymptotically to zero.

8 Results

The simulations were carried out by means of a position-tracking control involving a sinusoid with an amplitude of 0.08 m and angular frequency of 0.75 rad/s. The friction force F_A is represented in the simulations by means of the model of Gomes, proposed in [21]. The parameters of the friction model are described in [13]. The static neural networks were built with 30 neurons in the hidden layer.

The feedback gains used in the proposed controller were kept fixed with the values of $K_d = 5000s^{-1}$, $\lambda = 150s^{-1}$, and $K_p = 200s^{-1}$. For comparison purposes, we also performed a simulation using a classical PID controller and applied the proposed controller with the static neural network replaced by analytical functions. Such a controller uses only the viscosity friction term to compensate for the friction force in the piston, applying experimental parameters in Equation 4. The feedback gains values for PID are $K_p = 420$, $K_i = 2018$, $K_d = 0.9$, and were acquired according to the methodology described in [13]. Simulation results are shown in Figures 4 and 5, and Table 2 presents the RMSE results. Without the presence of a load disturbance, the results of MLP and WNN are similar, confirming that the present strategy keeps the effectiveness of the analytical controller, which uses analytical functions instead of static neural networks. According to [11], analytical functions are very hard to acquire. Applying a moderate load disturbance of 50 N, MLP neural networks present better error results than WNN, confirming that WNN is suitable only to local approximations and an online adjustment of the weights is necessary when a parametric variation occurs in the plant. MLP remains with effective results due to its characteristics as a global approximator.

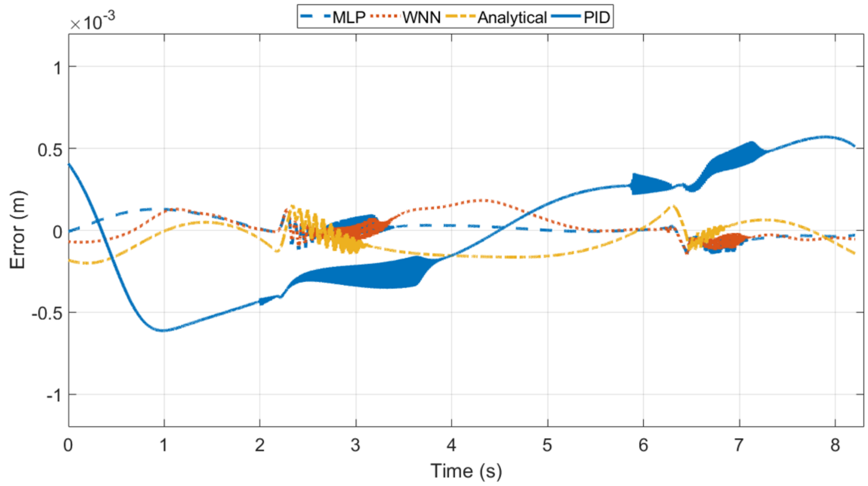

Fig. 4. Simulation of sinusoidal trajectory tracking control.

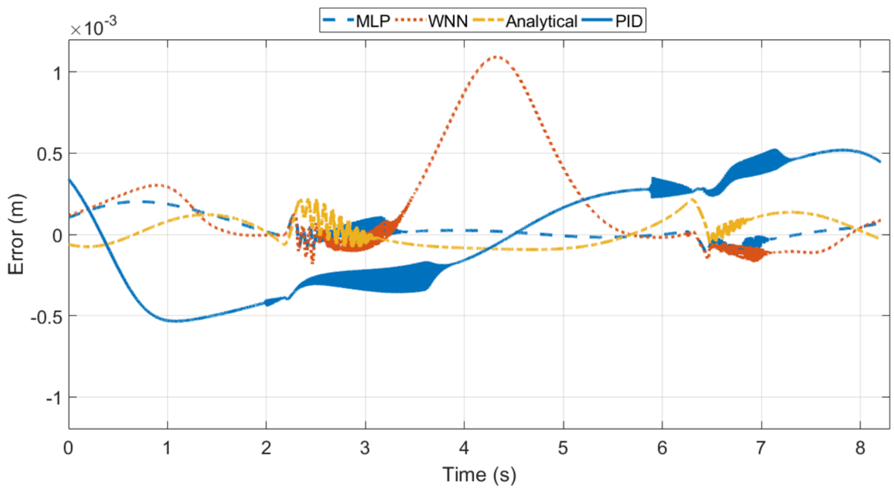

Fig. 5. Simulation of sinusoidal trajectory tracking control with FD = 50 N.

Table 2. Simulation position errors.

Disturbance (N)	Controller	Position error RMSE (m)
FD = 0	MLP	5.75×10^{-5}
	WNN	8.09×10^{-5}
	Analytical	10.68×10^{-5}
	PID	36.79×10^{-5}
FD = 50	MLP	8.14×10^{-5}
	WNN	36.73×10^{-5}
	Analytical	8.68×10^{-5}
	PID	34.58×10^{-5}

Experimental results regarding the plant are described in [11] and depicted in Figure 2, where the parameters are according to Table 1. Figures 6 and 7 illustrate the results, outlined in Table 3. Experimental results confirm previous simulation results. The proposed controller is effective in reducing the position error when compared with a traditional PID controller. However, when a disturbance force of 147 N is applied in the load, we can observe that the error results expose an important drawback that is present in model-based offline controllers: they are not able to deal with the presence of a high value for the load disturbance.

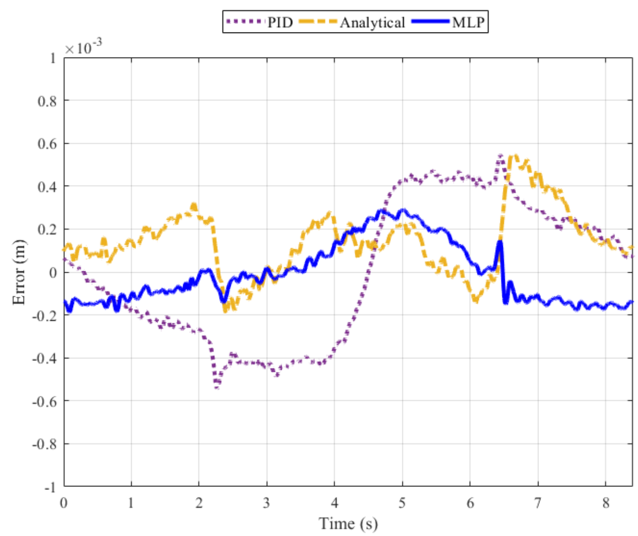

Fig. 6. Experimental result of sinusoidal trajectory tracking control.

Table 3. Experimental position errors.

Disturbance (N)	Controller	Position error RMSE (m)
FD = 0	MLP	8.3×10^{-5}
	Analytical	18×10^{-5}
	PID	31.2×10^{-5}
FD = 147	MLP	27.3×10^{-5}
	Analytical	34.9×10^{-5}
	PID	30×10^{-5}

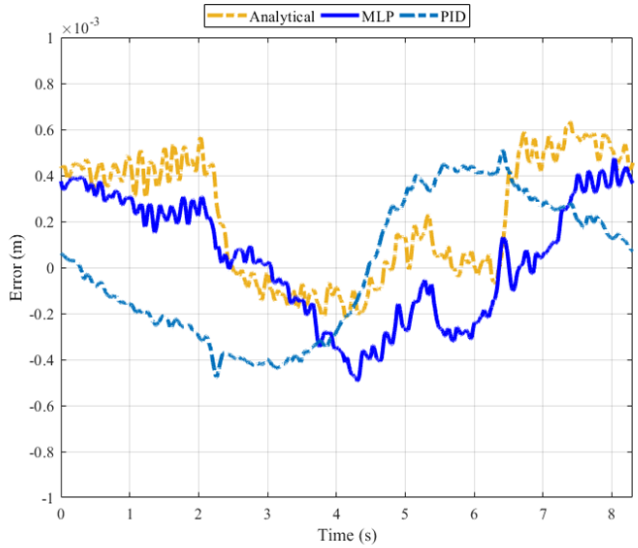

Fig. 7. Experimental result of sinusoidal trajectory tracking control with FD = 147 N.

9 Conclusion

In the present work, we propose the use of an offline trained static neural network to compensate for the nonlinearities present in the plant of a hydraulic actuator. This strategy aims to simplify and improve the application of feedback linearization-based control schemes to such systems, keeping the effectiveness of the controller. We showed by means of simulation and experimental results that the proposed controller is very effective in reducing position error compared with a traditional PID controller, with stability guarantees in the closed loop system. Future work will focus on the expansion of the proposed method to encompass high values of load disturbances in the hydraulic plant.

References

1. Watton, J.: Fundamentals of fluid power control, vol. 10. Cambridge University Press (2009)
2. Sun, C., Fang, J., Wei, J., Hu, B.: Nonlinear motion control of a hydraulic press based on an extended disturbance observer. IEEE Access **6**, 18,502–18,510 (2018). https://doi.org/10.1109/ACCESS.2018.2813317
3. Yang, X., Zheng, X., Chen, Y.: Position tracking control law for an electro-hydraulic servo system based on backstepping and extended differentiator. IEEE/ASME Transactions on Mechatronics **23**(1), 132–140 (2017). https://doi.org/10.1109/TMECH.2017.2746142

4. Luo, C., Yao, J., Gu, J.: Extended-state-observer-based output feedback adaptive control of hydraulic system with continuous friction compensation. Journal of the Franklin Institute **356**(15), 8414–8437 (2019). https://doi.org/10.1016/j.jfranklin.2019.08.015
5. Xinliang, L., Shan, J., Jing, Z., Wang, X.: Adaptive sliding mode position control of electro-hydraulic servo system with single-rod actuators. In: 2013 IEEE International Symposium on Robotic and Sensors Environments (ROSE), pp. 220–225. IEEE (2013). https://doi.org/10.1109/ROSE.2013.6698446
6. Ghazali, R., Ngadengon, R., Sam, Y.M., Rahmat, M., Hamzah, N., et al.: Chaotic trajectory tracking of an electro-hydraulic actuator system using discrete sliding mode control. In: 2011 IEEE International Conference on Control System, Computing and Engineering, pp. 500–506. IEEE (2011). https://doi.org/10.1109/ICCSCE.2011.6190577
7. Zhu, L., Wang, Z., Liu, Y., Song, W.: Sliding-mode dynamic surface control for mdf continuous hot pressing hydraulic system. In: 2016 Chinese control and decision conference (CCDC), pp. 2509–2514. IEEE (2016). https://doi.org/10.1109/CCDC.2016.7531407
8. Seo, J., Venugopal, R., Kenné, J.P.: Feedback linearization based control of a rotational hydraulic drive. Control Engineering Practice **15**(12), 1495–1507 (2007). https://doi.org/10.1016/j.conengprac.2007.02.009
9. Mintsa, H.A., Venugopal, R., Kenne, J.P., Belleau, C.: Feedback linearization-based position control of an electrohydraulic servo system with supply pressure uncertainty. IEEE Transactions on Control Systems Technology **20**(4), 1092–1099 (2011). https://doi.org/10.1109/TCST.2011.2158101
10. dos Santos Coelho, L., Cunha, M.A.B.: Adaptive cascade control of a hydraulic actuator with an adaptive dead-zone compensation and optimization based on evolutionary algorithms. Expert Systems with Applications **38**(10), 12,262–12,269 (2011). https://doi.org/10.1016/j.eswa.2011.04.004
11. Borges, F.A.P., Perondi, E.A., Cunha, M.A.B., Sobczyk, M.R.: A neural network-based inversion method of a feedback linearization controller applied to a hydraulic actuator. Journal of the Brazilian Society of Mechanical Sciences and Engineering **43**, 1–19 (2021). https://doi.org/10.1007/s40430-021-02957-y
12. Alexandridis, A.K., Zapranis, A.D.: Wavelet neural networks: A practical guide. Neural Networks **42**, 1–27 (2013). https://doi.org/10.1016/j.neunet.2013.01.008
13. Borges, F.A.P.: Controle em cascata de um atuador hidráulico utilizando redes neurais. Ph.D. thesis, Universidade Federal do Rio Grande do Sul (2017)
14. Slotine, J.J., Weiping, L.: Adaptive manipulator control: A case study. IEEE Transactions on Automatic Control **33**(11), 995–1003 (1988). https://doi.org/10.1109/9.14411
15. Oussar, Y., Dreyfus, G.: Initialization by selection for wavelet network training. Neurocomputing **34**(1-4), 131–143 (2000). https://doi.org/10.1016/S0925-2312(00)00295-2
16. Lima, L.B.d., Iano, Y., Oliveira, G.G.d., Vaz, G.C., Almeida, A.D.d., Motta, G.B., Villaça, G.M., Schwarz, M.O., Noritomi, P.Y.: Mathematical modeling: A conceptual approach of linear algebra as a tool for technological applications. In: Proceedings of the 7th Brazilian Technology Symposium (BTSym'21) Emerging Trends in Human Smart and Sustainable Future of Cities (Volume 1), pp. 239–248. Springer (2022)
17. Izario, D., Brancalhone, J., Iano, Y., de Oliveira, G.G., Vaz, G.C., Izario, K.: 5g-automation of vertical systems in the industry 4.0. In: Proceedings of the 7th

Brazilian Technology Symposium (BTSym'21) Emerging Trends in Human Smart and Sustainable Future of Cities (Volume 1), pp. 35–43. Springer (2022)
18. Bonello, D.K., Iano, Y., Neto, U.B., de Oliveira, G.G., Vaz, G.C.: A study about automated optical inspection: Inspection algorithms applied in flexible manufacturing printed circuit board cells using the mahalanobis distance method 1. In: Proceedings of the 7th Brazilian Technology Symposium (BTSym'21) Emerging Trends in Human Smart and Sustainable Future of Cities (Volume 1), pp. 198–212. Springer (2022)
19. Haykin, S.: Neural networks: a comprehensive foundation. Prentice Hall PTR (1998)
20. Fahlman, S.E., et al.: An empirical study of learning speed in back-propagation networks. Carnegie Mellon University, Computer Science Department Pittsburgh, PA, USA (1988)
21. Gomes, S.C.P., Da Rosa, V.S.: A new approach to compensate friction in robotic actuators. In: 2003 IEEE International Conference on Robotics and Automation (Cat. No. 03CH37422), vol. 1, pp. 622–627. IEEE (2003). https://doi.org/10.1109/robot.2003.1241663